AJNR

The added gradient echo pulse sequence technique: application to imaging of fluid in the temporomandibular joint.

K A Bell, J P Jones, K D Miller and D al-Refal

The Added Gradient Echo Pulse Sequence Technique: Application to Imaging of Fluid in the Temporomandibular Joint

Kenneth A. Bell,[1,2] Jerome P. Jones,[1] Kenneth D. Miller,[1] and Deena Al-Refai[1]

PURPOSE: To assess the value of an added gradient echo in the same pulse sequence with a T1-weighted spin echo for determining the presence of an abnormal fluid collection in the temporomandibular joint with no additional imaging time. **MATERIALS AND METHODS:** Using a standard T1-weighted sequence used in cine temporomandibular joint imaging, a readout gradient reversal was added and the resulting gradient echo collected. This image was compared with standard T1- and T2-weighted sequences, a short inversion recovery imaging sequence, and a small flip angle fast low-angle shot gradient-echo sequence. **RESULTS:** The T1-weighted spin echo preceeding the added gradient echo is not affected by the gradient reversal, but the additional gradient echo adds T2* contrast information that displays fluid as bright as and compares favorably with other fluid detection sequences. **CONCLUSION:** The added gradient-echo technique adds sensitivity for the detection of an abnormal increase in fluid in the temporomandibular joint without adding to the overall imaging time of a routine T1-weighted sequence.

Index terms: Temporomandibular joint, magnetic resonance; Magnetic resonance, technique

Magnetic resonance (MR) imaging has been shown by many investigators to be useful in evaluating temporomandibular joint (TMJ) dysfunction (1–44). Particularly helpful are "cine" studies where each image of a set is collected with the patient posed at a different degree of jaw opening (3–5, 20, 27). This image set is viewed in a cine display for evaluation of joint motion. Since several images may comprise a set, it is very desirable to keep the acquisition time for each image reasonably small while retaining adequate image quality. In particular, image contrast must be sufficient to evaluate the condylar marrow signal (to detect bone abnormalities such as avascular necrosis) and to detect the presence of abnormal fluid accumulations in the TMJ (which might account for patient discomfort as the jaw is opened). Thus, sensitivity to both fat and fluid is very desirable within the constraints of short imaging time.

The water-sensitive T2-weighted spin-echo and short inversion recovery imaging (STIR) sequences require too long a repetition time (TR) for reasonable scan times in cine studies. Both T1-weighted spin-echo and small tip angle gradient-echo sequences allow short scan times (on the order of 1 minute), with T1-weighted sequences giving strong marrow signal while the gradient-echo sequences give a relatively strong water signal. Running both these sequences gives the desired range of image contrasts through the range of jaw motion, but having to run two sequences at each cine pose doubles the examination time.

This increase in examination time can be avoided by combining both the spin echo and gradient echo into a single sequence. A basic single-echo spin-echo sequence is modified to produce an additional gradient echo by simply reversing the readout gradient after the spin echo has been collected and measuring the gradient echo which forms (see Fig. 1). This added gradient-echo (AGE) sequence simultaneously produces the strong marrow signal on the T1-weighted image along with the relatively strong

Fig. 1. A standard spin-echo sequence is diagrammed in *A*, while the same sequence with an added gradient echo (AGE) is shown in *B*. The added gradient echo is caused by a simple reversal of the readout gradient after the first echo has been read. The signal intensity of this gradient echo is given by

$$I_2 = I_1 \cdot exp[-(TE_2 - TE_1)/T2^*],$$

where I_1 is the signal intensity of the first echo (a standard spin echo), and TE_2-TE_1 is the time difference between the two echoes.

A   B
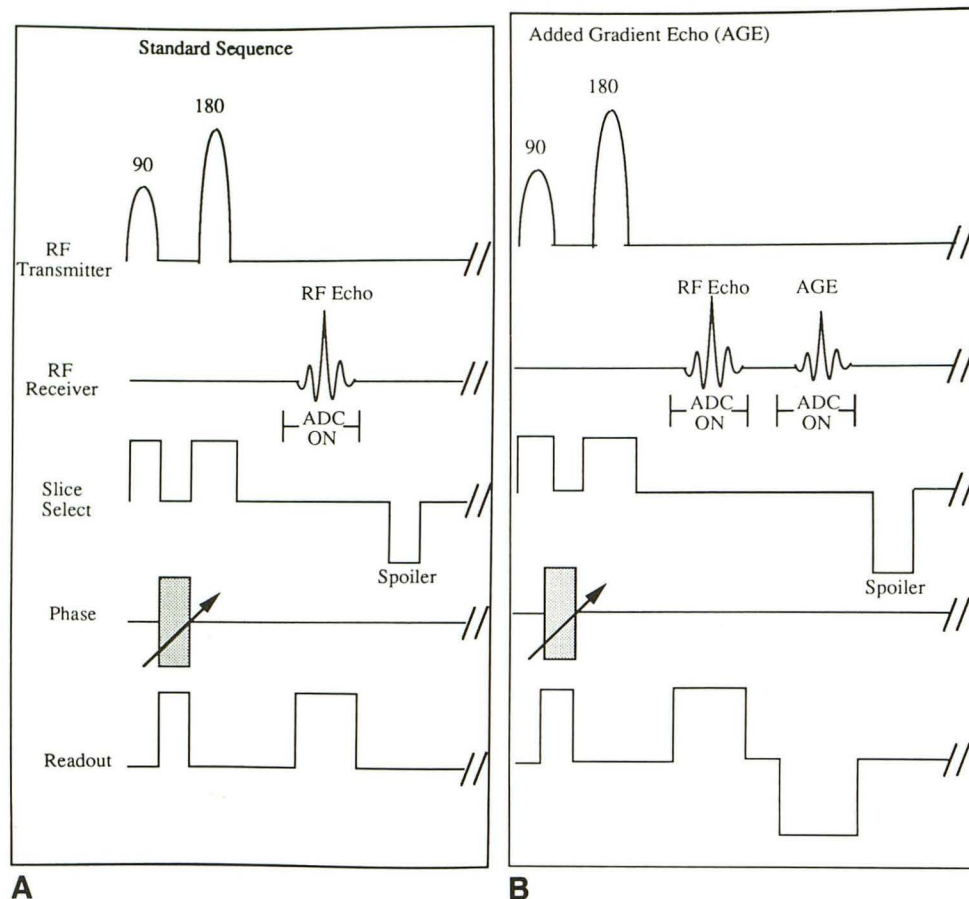
water signal from the gradient echo. Even better, both echoes are obtained in the same scan time as a single T1-weighted image having the same repetition time (TR), matrix size, and number of acquisitions. To our knowledge, such a simple technique has not been reported—that is, one which mixes standard spin echoes with gradient echoes (other sequences produce only one or the other).

Materials and Methods

All imaging was performed on either of two 1.5-T MR systems (Siemens Medical Systems, Iselin, NJ). Our basic approach was to determine the image contrast behavior of the AGE sequence and then apply it to clinical studies. Initially, a phantom containing oil, water, and water doped with a small amount of copper nitrate was imaged with standard T1- and T2-weighted sequences, the AGE sequence, a STIR sequence, and a small flip angle gradient-echo sequence, fast low-angle shot (FLASH). The TR, TE, and other parameter values used were the same as anticipated for use in clinical TMJ studies. (Since two 1.5-T systems which are different models were used, the exact values of TR and TE varied from one system to the other. The exact values used are listed in the figure captions.)

After some initial drawbacks were solved, the AGE sequence was incorporated into our routine cine TMJ imaging protocol, with 208 examinations being performed (and continuing to be performed). In addition, those TMJ studies in which abnormal fluid accumulation was clearly suggested by AGE were followed up with standard closed-mouth T2-weighted, STIR, or gradient-echo sequences known to be sensitive to fluids (17 of the 208 examinations). The images were then compared for their contrast properties and in one particular case, surgical verification was also available.

Results

Figure 2 shows the results obtained from the phantom of test tubes. Plain water was found to produce its strongest signal on the T2-weighted, FLASH 15°, and STIR sequences, while oil produced its strongest signal on the T1-weighted and AGE images. Thus, with these fluids, the AGE image was T1-weighted, at least for the TR and TE values used here.

Figure 3 shows a T1-weighted and AGE image from a normal patient study (closed mouth). Note that the AGE image shows low signal from condylar marrow, as expected, but is otherwise sim-
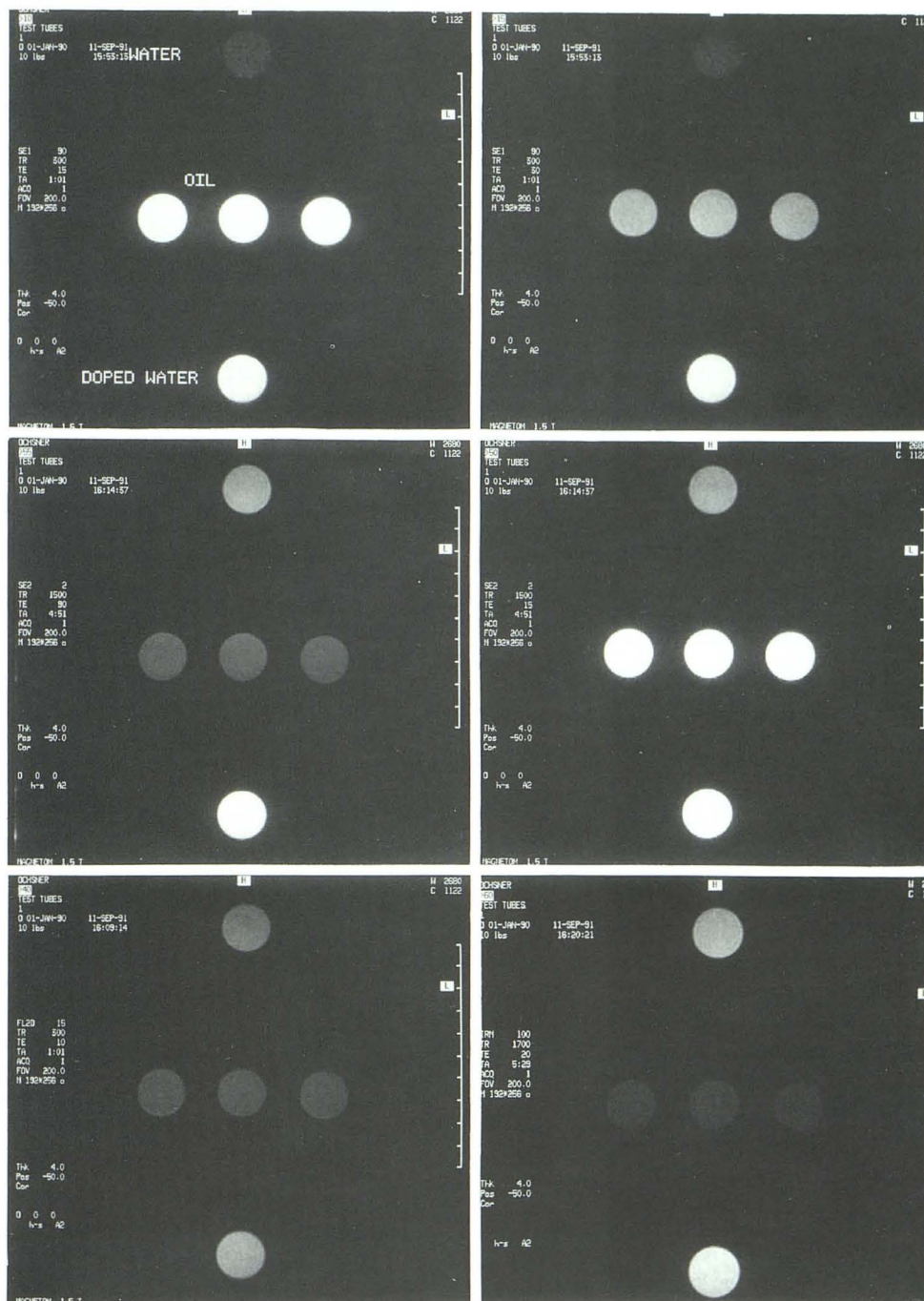
Fig. 2. Images from the phantom study. The upper row shows the two images from an AGE sequence; the T1-weighted image (300/15/1; TR/TE/acquisitions) on the left and the AGE image (300/30/1) on the right. The middle row shows the two echoes of a T2-weighted sequence (1500/15,90/1), and the bottom row shows a FLASH 15° image (300/10/1) on the left and a STIR image on the right (1700/20/1 with a TI of 100 msec).

ilar to the T1-weighted image in appearance. In particular, there is no strong signal from within the joint space; the normal tissues produce little signal on either image.

Figure 4 shows the results from a study in which the patient had a surgically verified cyst in the TMJ. All the sequences used with the phantom were run with this patient's jaw closed and resulted in images consistent with a cyst. Of particular interest is the observation that the AGE image shows the cyst with the same type of image contrast as the T2-weighted image (as well as the FLASH 15° and STIR images). Thus the AGE image is seen to show fluid more like a T2-weighted sequence, an observation that is somewhat surprising based upon its T1-weighting with the phantom. However, one must be careful which tissues are compared. When comparing fat and water, AGE is T1-weighted because all these materials are very homogeneous and produce a relatively strong echo. When comparing fluid to normal TMJ tissues, AGE is T2*-weighted be-
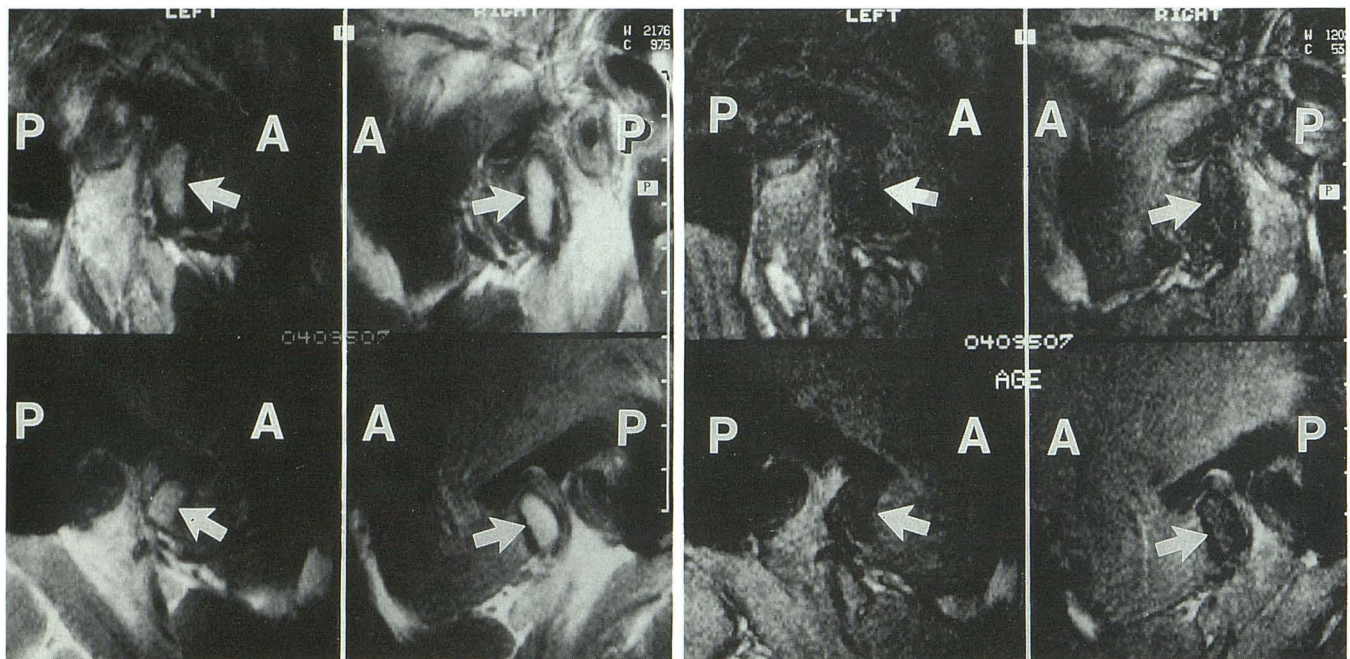
Fig. 3. A set of closed-mouth images in a normal patient study. Four T1-weighted (350/28/1) images are shown on the left and four AGE (350/40/1) images on the right, each presented as two adjacent sections from each side of the patient. Note that the condylar marrow (*arrows*) tends to be bright on T1-weighted images and dark on AGE images. Fluid in the temporomandibular joint is not normally observed on either image.

cause the normal TMJ tissues are much more inhomogeneous than fluid, and thus do not produce as strong a gradient-echo signal (compare Fig. 3 and Fig. 4).

Figure 5 is a case typical of the 16 other cases in which the AGE image suggested abnormal fluid collection. This patient complained of limited motion due to pain as her mouth opened. Again, the AGE image shows the same sense of contrast properties as the T2-weighted and other fluid-sensitive images, although the contrast is not as strong. Note also the small pocket of fluid buildup just anterior to the meniscus; such buildups are normally not observed and could account for the patient's pain on opening.

Discussion

AGE has been found to be a useful technique for obtaining images sensitive to TMJ fluid in cine studies. It is added to a T1-weighted spin-echo sequence, so it allows the usual T1-weighted images to be obtained. In addition, it allows tracking of the motion of the fluid during jaw opening, with no change in total examination time or spatial resolution. AGE also makes no unusual demands upon the gradient system and uses no additional radio frequency power; however, it should be noted that AGE does have some prop-

erties that should be considered before implementation: 1) fewer sections can be collected per TR due to the second echo; 2) the AGE image is both phase and frequency reversed, requiring an offline 180° rotation of the image before presentation (to produce correct labeling); 3) the AGE image is often too faint for otherwise low signal-to-noise imaging; and 4) the AGE image is more motion-sensitive than standard spin-echo images.

The contrast properties of AGE are essentially those of a standard spin echo, but multiplied by the $T2^*$ decay from the first (T1-weighted) echo to the gradient echo. AGE was implemented so that the added gradient echo occurred 10-12 msec (depending upon which MR unit was used) after the standard T1-weighted spin echo. Both the signal and contrast of this added gradient-echo image are the same as the conventional T1-weighted spin echo multiplied by any $T2^*$ contrast effects generated in the 10-12 msec between echoes. This additional $T2^*$ contrast is very important because it is what causes most tissues around a joint to produce minimal signal. Only the homogeneous tissues such as fat and fluids retain appreciable signal, so they stand out quite clearly on the AGE images. Since both fat and water tend to be bright on AGE images, they must be distinguished either by using the first
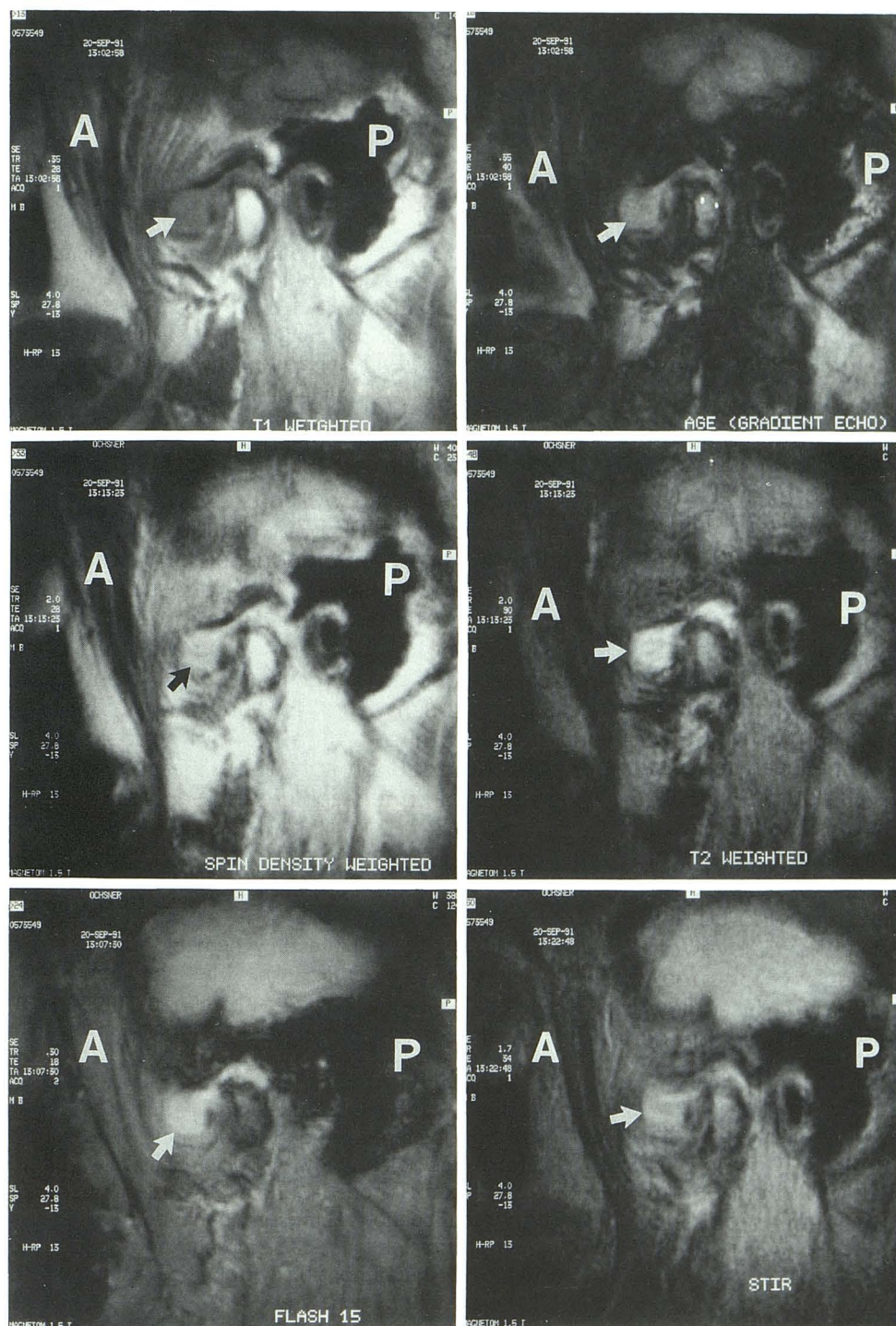
Fig. 4. Images from a patient diagnosed as having a cyst (*arrow*) which was surgically verified as secondary to synovial osteochondromatosis. The top row images are the T1-weighted and AGE images (350/28,40/1), the middle row images are those from the T2-weighted sequence (2000/28,90/1), and the bottom row are FLASH 15° (300/18/1) and STIR images (1700/34/1 with TI = 100 msec).

echo (which shows fat much brighter than water) or from a fat-suppression technique such as fat presaturation.

The AGE technique may also be helpful in several other possible applications, such as other types of cine-posing examinations, spine imaging to differentiate osteophytes from disk material, imaging of other joints, or locating hemosiderin deposits in the brain. In fact, any application where one desires gradient-echo contrast information is a possible application for AGE, and it can usually be applied to the T1-weighted image set. The primary drawbacks of AGE in other applications are the reduced number of sections per TR and the need for otherwise adequate signal-to-noise. AGE has proved to be of little use

Fig. 5. Images from a patient with temporomandibular joint pain on jaw opening. The top row images are closed-mouth T1-weighted (350/25/1), T2-weighted (2000/90/1), and AGE images (350/37/1) as viewed from left to right. The middle row images are all AGE images (350/37/1) at closed, moderately opened, and full open positions (left-to-right), while the bottom row images are the T1-weighted images (350/25/1) at the same section position and degrees of opening. The meniscus is seen to be anteriorly dislocated (*curved arrows*) and a fluid collection in the anterior part of the inferior joint space is also observed (*straight arrows*).

for axial spine images, thin section imaging, and/or half Fourier imaging due to poor signal-to-noise with resultant poor detectability of structures of interest. AGE also has the severe artifactual distortions that any gradient-echo sequence can have with patients who have dental braces or other metallic implants within the field of view. Despite these drawbacks, AGE may have a wide range of uses. The AGE technique is easily applied to any basic sequence: standard spin echo (as illustrated in this report), inversion recovery, or even a primary gradient-echo sequence such as FLASH; however, the clinical role for such AGE combinations has not yet been considered.

References

1. Adams HG, Riccio TJ. MR imaging scan protocols. In: Edelman RR, Hesselnik JR, eds. *Clinical magnetic resonance imaging.* Philadelphia: Saunders, 1990;1132–1152

2. Avrahami E, Schreiber R, Benmair J, Paltiel Z, Machtey J, Horowitz I. Magnetic resonance imaging of the temporo-mandibular joint and meniscus dislocation. *Br J Radiol* 1986;59:1153–1158

3. Burnett KR, Davis CL, Read J. Dynamic display of temporomandibular joint meniscus by using "fast-scan" MR imaging. *AJR* 1987; 149:959–962

4. Conway WF, Hayes CW, Campbell RL, Laskin DM. Temporomandibular joint motion: efficacy of fast low-angle shot MR imaging. *Radiology* 1989;172:821–826

5. Drace JE, Enzmann DR. Defining the normal temporomandibular joint: closed-, partially open-, and open-mouth MR imaging of asymptomatic subjects. *Radiology* 1990;177:67–71

6. Drace JE, Young SW, Enzmann DR. TMJ meniscus and bilaminar zone: MR imaging of the substructure—diagnostic landmarks and pitfalls of interpretation. *Radiology* 1990;177:73–76

7. Harms SE, Wilk RM. Magnetic resonance imaging of the temporomandibular joint. *Radiographics* 1987;7:521–542

8. Harms SE, Wilk RM, Wolford LM, Chiles DG, Milam SB. Temporomandibular joint: magnetic resonance imaging using surface coils. *Radiology* 1985;157:133–136

9. Hansson L-G, Westesson P-L, Katzberg RW, et al. MR imaging of the temporomandibular joint: comparisons of images of autopsy specimens made at 0.3 T and 1.5 T with anatomic cryosections. *AJR* 1989;152:1241–1244

10. Hasso AN, Christiansen EL, Alder ME. The temporomandibular joint. *Radiol Clin North AM* 1989;27:301–314

11. Helms CA, Doyle GW, Orwig D, McNeill C, Kaban L. Staging of internal derangements of the TMJ with magnetic resonance imaging: preliminary observations. *J Craniomandibular Disord* 1989;3:93–99

12. Helms CA, Gillespy T III, Sims RE, Richardson ML. Magnetic resonance imaging of internal derangement of the temporomandibular joint. *Radiol Clin North Am* 1986;24:189–192

13. Helms CA, Kaban LB, McNeill C, Dodson T. Temporomandibular joint: morphology and signal intensity characteristics of the disk at MR imaging. *Radiology* 1989;172:817–820

14. Helms CA, Kaplan P. Diagnostic imaging of the temporomandibular joint: recommendations for use of the various techniques. *AJR* 1990; 154:319–322

15. Herzog S, Mafee M. Synovial chondromatosis of the TMJ: MR and CT findings. *AJNR* 1990;11:742–745

16. Kaplan PA, Helms CA. Current status of temporomandibular joint imaging for the diagnosis of internal derangements. *AJR* 1989;152: 697–705

17. Kaplan PA, Tu HK, Williams SM, Lydiatt DD. The normal temporomandibular joint: MR and arthrographic correlation. *Radiology* 1987; 165:177–178

18. Katzberg RW. Temporomandibular joint imaging. *Radiology* 1989; 170:297–307

19. Katzberg RW, Bessette RW, Tallents RH, et al. Normal and abnormal temporomandibular joint: MR imaging with surface coil. *Radiology* 1986;158:183–189

20. Katzberg RW, Westesson P-L, Tallents RH, et al. Temporomandibular joint: MR assessment of rotational and sideways disk displacements. *Radiology* 1988;169:741–748

21. Kircos LT, Ortendahl DA, Mark AS, Arakawa M. Magnetic resonance imaging of the TMJ disc in asymptomatic volunteers. *J Oral Maxillofac Surg* 1987;45:852–854

22. Kneeland JB, Carrera GF, Ryan DE, Jesmanowicz A, Froncizw W, Hyde JS. MR imaging of a fractured temporomandibular disk prosthesis. *J Comput Assist Tomogr* 1987;11:199–200

23. Kneeland JB, Ryan DE, Carrera GF, Jesmanowicz A, Froncizw W, Hyde JS. Failed temporomandibular joint prostheses: MR imaging. *Radiology* 1987;165:179–181

24. Lieberman JM, Bradrick JP, Indresano AT, Smith AS, Ballone EM. Dermal grafts of the temporomandibular joint: postoperative appearance on MR images. *Radiology* 1990;176:199–203

25. Nance EP Jr, Powers TA. Imaging of the temporomandibular joint. *Radiol Clin North Am* 1990;28:1019–1031

26. Pollei SR, Schellhas KP. Magnetic resonance imaging of the temporomandibular joint. *Semin Ultrasound CT MR* 1990;11:346–361

27. Quemar JC, Bernard AM, Akoka S, Romdane H, Simon J, de Certaines JD. Magnetic resonance imaging of the TMJ: identification of anatomic elements by controlled movement and application to normal and pathologic clinical situations. *J Craniomandibular Disord* 1989;3:20–24

28. Rao VM, Babaria A, Manoharan A, et al. Altered condylar morphology associated with disc displacement in TMJ dysfunction: observations by MRI. *Magn Reson Imaging* 1990;8:231–235

29. Rao VM, Farole A, Karasick D. Temporomandibular joint dysfunction: correlation of MR imaging, arthrography, and arthroscopy. *Radiology* 1990;174:663–667

30. Roberts D, Schenck J, Joseph P, et al. Temporomandibular joint: magnetic resonance imaging. *Radiology* 1985;154:829–830

31. Schellhas KP. Internal derangement of the temporomandibular joint: radiologic staging with clinical, surgical, and pathologic correlation. *Magn Res Imaging* 1989;7:495–515

32. Schellhas KP, Wilkes CH. Temporomandibular joint inflammation: comparison of MR fast scanning with T1- and T2-weighted imaging techniques. *AJNR* 1989;10:589–594

33. Schellhas KP, Wilkes CH, El-Deeb M, Lagrotteria LB, Omlie MR. Permanent Proplast temporomandibular joint implants: MR imaging of destructive complications. *AJR* 1988;151:731–735

34. Schellhas KP, Wilkes CH, Fritts HM, Omlie MR, Heithoff KB, Jahn JA. Temporomandibular joint: MR imaging of internal derangements and postoperative changes. *AJNR* 1987;8:1093–1101

35. Schellhas KP, Wilkes CH, Fritts HM, Omlie MR, Heithoff KB, Jahn JA. Temporomandibular joint: MR imaging of internal derangement and postoperative changes. *AJR* 1988;150:381–389

36. Schellhas KP, Wilkes CH, Omlie MR, et al. The diagnosis of temporomandibular joint disease: two-compartment arthrography and MR. *AJNR* 1988;9:579–588

37. Schellhas KP, Wilkes CH, Omlie MR, et al. The diagnosis of temporomandibular joint disease: two-compartment arthrography and MR. *AJR* 1988;151:341–350

38. Schwaighofer BW, Tanaka TT, Klein MV, Sartoris DJ, Resnick D. MR imaging of the temporomandibular joint: a cadaver study of the value of coronal images. *AJR* 1990;154:1245–1249

39. Shellock FG, Pressman BD. Dual-surface-coil MR imaging of bilateral temporomandibular joints: improvements in the imaging protocol. *AJNR* 1989;10:595–598

40. Walter E, Hüls A, Schmelzle R, Küper K, Kalender WA. CT and MR imaging of the temporomandibular joint: *Radiographics* 1988;8: 327–348

41. Westesson P-L, Katzberg RW, Tallents RH, Sanchez-Woodworth RE, Svensson SA, Espeland MA. Temporomandibular joint: comparison of MR images with cryosectional anatomy. *Radiology* 1987;164:59

42. Wilk RM, Harms SE. Temporomandibular joint: multislab, three-dimensional Fourier transformation MR imaging. *Radiology* 1988; 167:861–863

43. Wilk RM, Harms SE, Wolford LM. Magnetic resonance imaging of the tempormandibular joint using a surface coil. *J Oral Maxillofac Surg* 1986;44:935–943

44. Wright SM, Wright RM. Bilateral MR imaging with switched mutually coupled receiver coils. *Radiology* 1989;170:249–255